Clamping Force of A Multilayered Cylindrical Clamp with Internal Friction

Bo-Hua Sun[1] and Xiao-Lin Guo[2]

[1]*School of Civil Engineering & Institute of Mechanics and Technology*
[2]*School of Sciences & Institute of Mechanics and Technology*
Xian University of Architecture and Technology, Xian 710055, China
Corresponding author: B.H.S. email: sunbohua@xauat.edu.cn

Holding an object by clamping force is a fundamental phenomena, layered or laminated architectures with internal sliding features are essential mechanism in natural and man-made structural system. In this paper, we combine the layered architecture and clamping mechanism to form a multilayered clamp and study the clamping force with internal friction. Our investigations show that the clamping force and energy dissipation are very much depend on the number of layers, its geometry and elasticity, as well as internal friction. The central goal of studying the multilayered clamp is not only to predict the clamping force, but also as a representative case to help finding some clue on the universal behaviours of multilayered architectures with internal friction.

Keywords: Clamping force, multilayer clamp, curvature, bending, friction, dissipation, deflection

I. INTRODUCTION

Holding an object by clamping force is a fundamental process for functional structures in natural and man-made systems. Examples encompass different applications, such as medical clips, glass frame, hairband, headphone as well as robotic hand (as shown in Fig.1.)

FIG. 1: Some examples of using clamping force.

Everyone may have the experience of holding an egg in their hand, and in order to prevent the egg from falling, you must apply enough clamping force, but the clamping force must also be just right, otherwise the egg will be crushed. Similarly, if you want to design a robotic hand to grasp objects that are very easy to break, the control of the clamping force is very important. Therefore, accurately predicting the clamping force is a problem worth to be studied.

To have a better strength and a good flexibility, layered or laminated architectures with internal sliding features are essential mechanism in natural and man-made structural system [1, 2]. For example, scaled skins are a very common structure in both the animal kingdom and engineering applications, such as lizards, fish, leaf springs, scaled armour, pangolin and books [1–14].

In this paper, we combine the layered architecture and clamping mechanism to form a multilayered clamp and study the multilayered cylindrical clamp with internal friction. In the deformation of the layered structures/system, the interactions between layers play a central role in controlling the overall mechanical performance of the system, in particular the interlayered friction is crucial to the response of elastic system. As pointed by Poincloux et al. [1], it is a great challenging to predict how the microscopic architecture and interlayer interactions of a layered mechanical system give rise to a specific macroscopic constitutive response, especially for large deformations.

In this paper, In Section 1 first highlight the layered architectures and its challenges. In Section 2 introduce assumptions of theory and derive the implicit clamping force-deformation relation for a multilayered clamp without internal friction. In Section 3, we derive the explicit clamping force-deformation relation for a multilayered clamp without internal friction. In Section 4, we derive the explicit clamping force-deformation relation for a multilayered clamp with internal friction. In Section 5, we derive energy dissipation during loading-unloading cycle. In Section 6, some numerical results will be carried for different parameters. Finally, conclusions and perspectives are proposed.

II. FORMULATIONS AND IMPLICIT REPRESENTATION OF CLAMPING FORCE WITHOUT INTERNAL FRICTION

Consider a clamp in Fig.2 whose layout is denoted $[\underbrace{h...h}_{n}]$. The clamp length is L and width is W, top/bottom hardcover thickness are c. The clamp has n layers and each layer thickness is h, hence the clamp dimensions is $L \times W \times (nh)$, where nh is total thickness

(height). The Young's modular and Poisson ratio are E and ν, respectively.

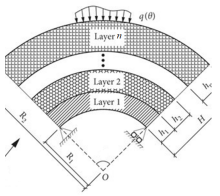

FIG. 2: Multilayers layout with layer thickness $h_1 = h_2 ... = h$.

For investigation of the clamp with interlayer friction, following assumptions will be adopted: 1. The Kirchhoff hypothesis is applied; 2. Each layer is inextensible; 3. No delamination; 4. Interlayers can slide with friction; 5. In cylindrical bending.

For a multilayers plate with n layers having equal thickness h, the total bending stiffness is nB for zero interfacial friction, and n^3B for infinite interfacial friction. What is the bending stiffness of a multilayers with internal friction ?

$$\text{Bending stiffness} = \begin{cases} nB & \text{with zero friction} \\ What\,? & \text{with finite friction} \\ n^3B & \text{with infinite friction} \end{cases}$$

We can estimate that the stiffness of the multilayers must be bounded by scale of nB and n^3B, where the bending stiffness of a single layer, $B = \frac{Eh^3W}{12(1-\nu^2)}$. The problem is how to quantitatively determine the effective bending stiffness of the multilayers with internal friction.

The problem of clamping force-deformation is illustrated in Fig.3.

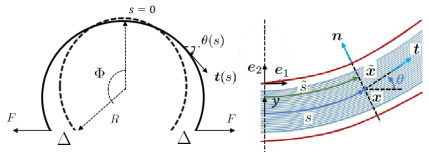

FIG. 3: Deformation under horizontal clamping force F. Tangent angle θ versus arc length s. $\tilde{\boldsymbol{x}}(s,y) = \boldsymbol{x}(s) + \boldsymbol{n}(s)y$, where $\boldsymbol{x}(s) = x_1(s)\boldsymbol{e}_1 + x_2(s)\boldsymbol{e}_2$ is a reference inextensible planar curve of centerline, $\boldsymbol{n}(s)$ is the unit normal vector to the centerline. The arc length $\tilde{s}$ on the offset curve is given by $d\tilde{s} = ds\sqrt{1 + 2y\kappa + y^2\kappa^2} = (1 + y\kappa)ds$.

The formulations of this problem is similar to a book with internal friction [1, 14], whose balance equation can be applied to current problem. In Fig. 3, if the horizontal clamping force F is considered, Sun et al.[14] derived a balance equation by using variational principal, $\frac{dM}{ds} + \frac{d}{ds}(\kappa\frac{dM}{d\kappa}) - 2F\sin\theta(s) = 0$, where bending moment is $M = \frac{B}{h}\ln\frac{1+\frac{nh}{2}\kappa}{1-\frac{nh}{2}\kappa}$, and curvature is $\kappa = \frac{d\theta}{ds}$. Hence, we have the balance equation as follows

$$\frac{nB\theta''}{[1-(\frac{nh}{2}\theta')^2]^2} - F\sin\theta = 0, \tag{1}$$

and the boundary conditions $\theta(L/2) \equiv \theta_0$ and $\theta'(L/2) = 1/R$, where $L = 2R\Phi$, and the bending stiffness $B = \frac{Eh^3W}{12(1-\nu^2)}$.

The first integral of Eq. 1 is

$$\frac{2B}{nh^2}\frac{1}{1-(\frac{nh}{2}\theta')^2} + F\cos\theta = C, \tag{2}$$

where C is integration constant and can be determined by the boundary conditions at $s = L/2$, namely $C = \frac{2B}{nh^2}\frac{1}{1-(\frac{nh}{2R})^2} + F\cos\theta_0$

The first integral of Eq. 1 is calculated as follows:

$$\frac{2B}{nh^2}\frac{1}{1-(\frac{nh}{2}\theta')^2} + F\cos\theta = \frac{2B}{nh^2}\frac{1}{1-(\frac{nh}{2R_s})^2} + F\cos\theta_0, \tag{3}$$

This can be rewritten as

$$\frac{ds}{R} = \frac{nh}{2R}d\theta\sqrt{\frac{\frac{2}{n}(\frac{R}{h})^2 + \epsilon[1-(\frac{nh}{2R})^2](\cos\theta_0 - \cos\theta)}{\frac{n}{2} + \epsilon[1-(\frac{nh}{2R})^2](\cos\theta_0 - \cos\theta)}}, \tag{4}$$

where the small parameter ϵ is $\epsilon = \frac{FR^2}{B}$.

Equation (4) is substituted into the non-elongation condition $\int_0^{L/2} ds = R\Phi$ of the elastomer, where $L = 2R\Phi$. The non-elongation condition can be written as

$$\frac{2}{nh}\int_0^{L/2} ds = \int_0^{\theta_0} d\theta\sqrt{\frac{\frac{2}{n}(\frac{R}{h})^2 + \epsilon[1-(\frac{nh}{2R})^2](\cos\theta_0 - \cos\theta)}{\frac{n}{2} + \epsilon[1-(\frac{nh}{2R})^2](\cos\theta_0 - \cos\theta)}}, \tag{5}$$

For any parameter $\epsilon = \frac{FR^2}{B}$, using symbolic computation software such as Maple, we can find the exact solution $\Phi = f(\theta_0)$ of Eq. (5) in terms of elliptic functions. Since the solution $\Phi = f(\theta_0)$ takes few pages long, we would not display it here.

Since we only know the initial opening angle Φ and not the inclination angle θ_0 of the deformation. The exact solution $\Phi = f(\theta_0)$ must be inverted to obtain the analytical expression of the deformation inclination θ_0 expressed by the initial opening angle Φ, i.e., $\theta_0 = \theta_0(\Phi)$.

Although we obtained the exact solution $\Phi = f(\theta_0)$, to the best of the authors' knowledge, it is almost impossible to obtain the inverse of the exact solution. Thus, we do not seek an exact solution. For convenience, we determine whether an approximate treatment is feasible.

Expression (4) is expanded for a small parameter $\epsilon = \frac{FR^2}{B}$, and the first-order approximation is as follows:

$$\frac{ds}{R} \approx d\theta\left\{1 - \frac{\epsilon}{n}[1-(\frac{nh}{2R})^2]^2(\cos\theta_0 - \cos\theta)\right\} + O\left(\epsilon^2\right). \tag{6}$$

Expression (6) is substituted into the non-elongation condition $\int_0^{L/2} ds = R\Phi$ of the elastomer, where $L = 2R\Phi$.

The non-elongation condition can be written as

$$\frac{1}{R}\int_0^{L/2} ds = \int_0^{\theta_0} d\theta \left\{1-\frac{\epsilon}{n}[1-(\frac{nh}{2R})^4](\cos\theta_0-\cos\theta)\right\}+O\left(\epsilon^2\right). \tag{7}$$

and thus,

$$\Phi=\theta_0-\frac{\epsilon}{n}[1-(\frac{nh}{2R})^2]^2(-\sin\theta_0+\theta_0\cos\theta_0)+O\left(\epsilon^2\right). \tag{8}$$

Expression (8) is a first-order approximate result derived naturally by rigorous mathematics.

Based on the deformation in Fig. 3, the horizontal deformation relationship is

$$x(\frac{L}{2})-x(0)=\int_0^{L/2}\cos\theta(s)ds=R\sin\Phi+\Delta, \tag{9}$$

where Δ represents the horizontal displacement driven by force F. Expression (6) is substituted into (9) to obtain

$$x(\frac{L}{2})-x(0)\approx R\sin\Phi+\Delta \approx R\int_0^{\theta_0}\cos\theta(s)d\theta\left\{1-\frac{\epsilon}{n}[1-(\frac{nh}{2R})^2]^2(\cos\theta_0-\cos\theta)\right\}. \tag{10}$$

This can be written as

$$\sin\theta_0+\frac{1}{2}\frac{\epsilon}{n}[1-(\frac{nh}{2R})^2]^2(\theta_0-\sin\theta_0\cos\theta_0)=\sin\Phi+\frac{\Delta}{R}. \tag{11}$$

Expression (8) is substituted into the above formula to obtain

$$\sin\theta_0+\frac{1}{2}\frac{\epsilon}{n}[1-(\frac{nh}{2R})^2]^2(\theta_0-\sin\theta_0\cos\theta_0) =\sin\left[\theta_0+\frac{\epsilon}{n}[1-(\frac{nh}{2R})^2]^2\left(\sin\theta_0-\theta_0\cos\theta_0\right)\right]+\frac{\Delta}{R}. \tag{12}$$

Expanding the both sides to the first-order term of ϵ leads to

$$\sin\theta_0+\frac{1}{2}\frac{\epsilon}{n}[1-(\frac{nh}{2R})^2]^2(\theta_0-\sin\theta_0\cos\theta_0) =\frac{\Delta}{R_s}+\sin\theta_0-\frac{\epsilon}{n}[1-(\frac{nh}{2R})^2]^2\left(\theta_0\cos\theta_0-\sin\theta_0\right)\cos\theta_0. \tag{13}$$

We can obtain the following expression for $\epsilon=FR^2/B$:

$$\frac{FR^2}{B}=\frac{n}{[1-(\frac{nh}{2R})^2]^2}\frac{\Delta}{R}K(\theta_0), \tag{14}$$

where $K(\theta_0)=\left[\frac{\theta_0}{2}-(\frac{3}{2}\sin\theta_0-\theta_0\cos\theta_0)\cos\theta_0\right]^{-1}$.

III. EXPLICIT REPRESENTATION OF CLAMPING FORCE - DEFORMATION RELATION WITHOUT INTERNAL FRICTION

Although we have obtained the relation in Eq.14, however, the clamping force - deformation relation is not an explicit format of opening angle Φ. To resolve the problem, we need to find the inversion of the derived relation in Eq.8, namely $\Phi\approx\theta_0-\frac{\epsilon}{n}[1-(\frac{nh}{2R})^2]^2(-\sin\theta_0+\theta_0\cos\theta_0)$. Unfortunately, it is impossible to find its exact inversion. Based on success of [15, 16], a fair good approximate inversion can be obtained as follows

$$\theta_0\approx\Phi-\frac{\epsilon}{n}[1-(\frac{nh}{2R})^2]^2(\sin\Phi-\Phi\cos\Phi). \tag{15}$$

Substituting Eq.15 into Eq.14 and expanding to the 1st order of ϵ, and leads to

$$\frac{FR^2}{B}=\frac{n}{[1-(\frac{nh}{2R})^2]^2}\frac{\Delta}{R}K(\Phi), \tag{16}$$

where $K(\Phi)=\left[\frac{\Phi}{2}-(\frac{3}{2}\sin\Phi-\Phi\cos\Phi)\cos\Phi\right]^{-1}$. Eq.16 is the clamping force - deformation relation for the multilayered open clamp without internal friction.

IV. EXPLICIT REPRESENTATION OF CLAMPING FORCE - DEFORMATION RELATION WITH INTERNAL FRICTION

To include the effect of internal friction, the dissipation analysis must be done, which has been studied by Poincloux [1], who obtained effective bending stiffness $K_{\rm Lin}=nB\left(1\pm\frac{3\mu nh}{2L}\right)$, where μ is friction coefficient, the + sign for loading (from the natural state to deformed state) and − sign for unloading (from deformed state to the natural state). Replace nB by $K_{\rm Lin}$ and will produce

$$\frac{F^{\pm}R^2}{B}=n\frac{1\pm\frac{3}{2}\mu\frac{nh}{L}}{[1-(\frac{nh}{2R})^2]^2}\frac{\Delta}{R}K(\Phi), \tag{17}$$

where $K(\Phi)=\left[\frac{\Phi}{2}-(\frac{3}{2}\sin\Phi-\Phi\cos\Phi)\cos\Phi\right]^{-1}$. Eq.17 is the clamping force - deformation relation for the multilayered open clamp with internal friction.

For a single layer clamp $n=1$ without friction $\mu=0$, and overall slender, $nh/(2R)\ll 1$, the expression in Eq.17 will be reduced to, $\frac{FR^2}{B}=K(\Phi)\frac{\Delta}{R}$, which is the result obtained by Yoshida and Wada [15] for elastic circular snap fit.

V. ENERGY DISSIPATION DURING LOADING-UNLOADING CYCLE

The expression of F for loading and unloading in Eq. 17 yields the following prediction for the energy dissipat-

ed during one cycle:

$$D = \int_0^{\Delta} F^+ d\Delta - \int_0^{\Delta} F^- d\Delta = \frac{3}{2}\frac{\mu B h}{RL}\frac{1}{[1-(\frac{nh}{2R})^2]^2}\left(\frac{n\Delta}{R}\right)^2 K(\Phi) \qquad (18)$$

For given opening angle Φ, the energy dissipation D is proportional to the n^2, which reveals a simple mechanism where the energy dissipated per cycle can be made to vary by a large amount; this could be harnessed to design new classes of low-cost and efficient damping devices.

VI. NUMERICAL SIMULATIONS

For numerical validation, we consider the surface of an acrylic cylinder with radius $R = 10 \sim 23[mm]$ with a thin oriented polypropylene sheet of thickness $h = 0.00143[m]$ to ensure uniform frictional interactions with the shell, with friction coefficient $\mu = 0.52$, length $L = 0.11[m]$, width $W = 0.03[m]$, the Young modulus $E = 2.4 \times 10^9[N/m^2]$, the Passion ratio $\nu = 0.44$ and single layer bending stiffness $B = Eh^3W/[12(1-\nu^2)] = 0.021757 \times 10^{-4}[Nm^2]$.

The dimensionless clamping force $P = \frac{FR^3}{nB\Delta}[1-(\frac{nh}{2R})^2]^2/[1+\frac{3}{2}\mu\frac{nh}{L}]$ of Eq. 17 is depicted in Fig.4, which shows that the P is decreased with the increase of the opening angle.

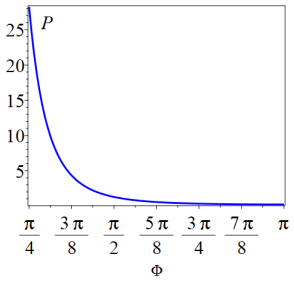

FIG. 4: $P-\Phi$ profile, where the dimensionless parameter $P = \frac{FR^3}{nB\Delta}[1-(\frac{nh}{2R})^2]^2/[1+\frac{3}{2}\mu\frac{nh}{L}]$.

If we set the opening angle $\Phi = 2.3$, the clamping force-deformation ration F/Δ is increasing with the increasing with the number of layers n, which is depicted in Fig.5. If we set the number of layers $n = 20$, the clamping force-deformation ration F/Δ is linear proportional to the friction coefficient μ, which is depicted in Fig.6. The $F/\Delta - \mu$ profile is a straight line. If we set the number of layers $n = 20$, the clamping force-deformation ration F/Δ is deceasing with the increasing of radius R, which is depicted in Fig.7.

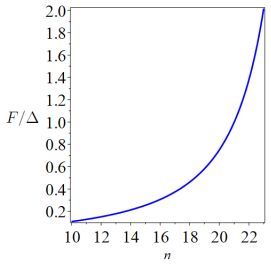

FIG. 5: $F/\Delta - n$ profile, for case of the opening angle $\Phi = 2.3$.

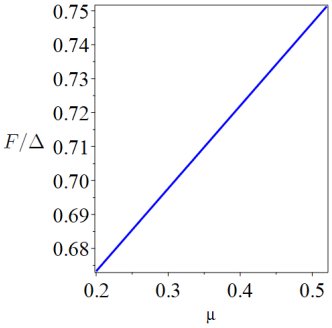

FIG. 6: $F/\Delta - \mu$ profile, for the case of layers number $n = 20$.

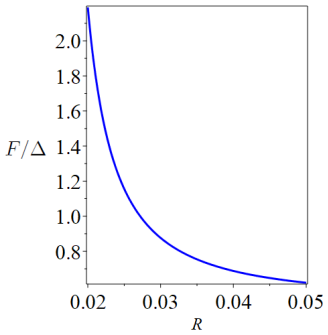

FIG. 7: $F/\Delta - R$ profile, for the case of layers number $n = 20$.

VII. CONCLUSIONS AND PERSPECTIVES

We studied the clamping force of the multilayer clamp and derived the expression of the clamping force and energy dissipation when considering friction, and the results showed that the number of layers, friction coefficient and radius all have an impact on the clamping force. When considering internal friction, the energy dissipation within per loading-unloading cycle can be made to vary by a considerable amount. The study here helps to understand the mechanical interactions behavior in between of geometry, friction and elasticity.

ACKNOWLEDGMENTS

This work was supported by Xi'an University of Architecture and Technology (Grant No. 002/2040221134).

[1] S. Poincloux, T. Chen, B. Audoly and P.M. Reis, Bending response of a book with internal friction, Phy.Rev.Lett. 126, 218004 (2021).
[2] J. R. Vinson, Sandwich structures, Appl. Mech. Rev. 54, 201 (2001).
[3] A. Jackson, J. F. Vincent, and R. Turner, The mechanical design of nacre, Proc. R. Soc. B 234, 415 (1988).
[4] Z. Tang, N. A. Kotov, S. Magonov, and B. Ozturk, Nanostructured artificial nacre, Nat. Mater. 2, 413 (2003).
[5] Z. Yin, F. Hannard, and F. Barthelat, Impact-resistant nacre-like transparent materials, Science 364, 1260 (2019).
[6] G. Wang, Z. Dai, J. Xiao, S. Z. Feng, C. Weng, L. Liu, Z. Xu, R. Huang, and Z. Zhang, Bending of multilayer van der Waals materials, Phys. Rev. Lett. 123, 116101 (2019).
[7] B. J. Bruet, J. Song, M. C. Boyce, and C. Ortiz, Contact kinematics of biomimetic scales, Nat. Mater. 7, 748 (2008).
[8] H. Ali, H. Ebrahimi, and R. Ghosh, Frictional Damping from biomimetic scales, Sci. Rep. 9, 14628 (2019).
[9] J. H. Griffin, Shear Sliding Failure of the Jointed Roof in Laminated Rock Mass, Int. J. Turbo Jet Engines 7, 297 (1990).
[10] F. Badrakhan, Slip damping in vibrating layered beam and leaf springs: energy dissipated and optimum considerations, J. Sound Vib. 174, 91 (1994).
[11] M. Osipenko, Y. Nyashin, and R. Rudakov, A contact problem in the theory of leaf spring bending, Int. J. Solids Struct. 40, 3129 (2003).
[12] S. Hansen and R. Spies, Structural damping in laminated beams due to interfacial slip, J. Sound Vib. 204, 183 (1997).
[13] H. M. Sedighi, K. H. Shirazi, and K. Naderan-Tahan, Stick-slip vibrations of layered structures undergoing large deflection and dry friction at the interface, J. Acoust. Vib. 135, 061006 (2013).
[14] Sun, B.H; Dang, W.; Liu, X.T.; Guo, X.L., Cylindrical Bending of A Hardcover Book with Internal Friction. Preprints 2022, 2022040178 (doi: 10.20944/preprints202204.0178.v1).
[15] K. Yoshida and H. Wada. Mechanics of a snap fit. Phys. Rev. Lett. **125**, 194301 (2020).
[16] X.L. Guo and B.H. Sun, Assembly and disassembly mechanics of a cylindrical snap fit. Preprints 2022, 2022010076 (doi: 10.20944/preprints202201.0076.v1).